Development of renin expression in the mouse kidney

A Sauter[1,2], K Machura[1,2], B Neubauer[1], A Kurtz[1] and C Wagner[1]

[1]*Institut für Physiologie der Universität Regensburg, Regensburg, Germany*

During metanephric kidney development, renin is expressed in the walls of larger intrarenal arteries, but is restricted to the terminal part of the preglomerular arterioles in the adult kidney. Our study describes the three-dimensional development of renin expression in mouse kidneys during fetal and postnatal life. Renin immunoreactivity first appeared at day 14 of development in the cells expressing α-smooth muscle actin (αSMA) in the arcuate arteries. Before adulthood, the branching of the arcuate arterial tree increased exponentially and renin expression shifted from proximal to distal parts of the tree. Renin expression at branching points or in the cones of growing vessels was not seen. Instead, renin expression appeared after vessel walls and branches were already established, disappeared a few days later, and remained only in the juxtaglomerular regions of afferent arterioles. In these arterioles, coexpression of renin and αSMA disappeared gradually, with the terminal cells expressing only renin. At all stages of kidney development, renin expression among comparable vessel segments was heterogeneous. Renin expression remained stable after it reached the terminal parts of afferent arterioles.

Kidney International (2008) **73,** 43–51; doi:10.1038/sj.ki.5002571; published online 26 September 2007

KEYWORDS: renal vessel; α-smooth muscle actin; juxtaglomerular cell; branching; three-dimensional reconstruction

Correspondence: *C Wagner, Institut für Physiologie, Universität Regensburg, Regensburg D-93040, Germany.*
E-mail: charlotte.schmid@vkl.uni-regensburg.de

[2]These authors contributed equally to this work

Received 24 May 2007; revised 28 June 2007; accepted 1 August 2007; published online 26 September 2007

In the mammalian kidney, the protease renin is predominantly produced and stored in cells of the media layer of afferent arterioles at the last branching point leading to the glomerular capillary network. Usually renin-producing cells, which develop an epithelioid shape due to the content of numerous renin-storage granules, replace the typical smooth muscle cells in the media layer and form the walls of the vessels entering the glomeruli. Media cells of the efferent arterioles or extraglomerular mesangial cells only rarely express renin, mainly depending on the animal species.[1] The typical juxtaglomerular position of renin-producing cells is the final destination of a highly plastic expression of renin during the development of the kidney. A body of evidence suggests that the developmental changes of intrarenal renin expression occur along the same pattern in all mammals including man.[2–12] This phenomenon, which so far has been studied in more detail for mouse[6] and rat kidneys,[7] appears to start with renin expression in the developing renal artery, interlobar arteries, and arcuate arteries. With the development of interlobular arteries, renin expression starts there and disappears in the bigger vessels. Renin expression is then found in newly developed afferent arterioles and it disappears from interlobular arteries around the time of birth in mice and rats. With ongoing postpartal maturation of the kidneys, renin expression becomes more and more restricted to the terminal part of the afferent arterioles, that is, the juxtaglomerular position. The mechanisms switching renin expression on and off in the various segments of the developing intrarenal arterial vasculature are unknown. The same holds true for the striking juxtaglomerular position of renin expression in the adult kidney, although there are hypotheses that still await functional proof.[13,14] The functional meaning of this characteristic shift of renin expression in the developing mammalian kidney is also less clear. It has been hypothesized that renin expression could somehow be of relevance for the branching sites of the intrarenal vasculature, because in the adult rat kidney, renin expression is besides the juxtaglomerular position predominantly found at branching points of the vasculature.[15]

The regulation of the development of the precisely organized preglomerular arterial network is also poorly understood. There is some evidence that both vasculogenesis and angiogenesis contribute to the formation of the intrarenal vessel tree.[16]

One methodical limitation in the understanding of intrarenal vessel formation and the developmental switch turning renin expression on and off is that vessels and renin expression develop in three dimensions, while histological sectioning only allows a two-dimensional view, necessitating extrapolation of the third dimension.

We were therefore interested in obtaining a three-dimensional view of vessel formation and of renin expression in the developing mouse kidney directly. With this approach, we first aimed to address several basic questions, such as where and how does renin first appear during kidney development? Is renin located primarily at branching sites during vessel development? How constant is the expression of renin in comparable vessel segments? Is there a continuous shift of renin expression from bigger to smaller vessels?

Apart from these defined questions, we also aimed to characterize renin expression in the developing normal mouse kidney to establish a reference system for future investigations of mice with defined genetic defects utilized to identify relevant gene products involved in the developmental regulation of renin expression.

To reach these defined goals, we reconstructed the intrarenal vascular tree and the regions of renin expression from serial sections of mouse kidneys of different fetal and postpartal states of development.

RESULTS

Development of the preglomerular arterial tree

We used α-smooth muscle actin (αSMA) immunoreactivity as an indicator for arterial preglomerular vessels. At day 12 of embryonic development, we found a bud protruding into the metanephric mesenchyme, likely reflecting the developing renal artery (not shown).

One day later (day E13), the renal artery was clearly visible (Figure 1a). It had divided into two branches, likely reflecting the interlobar arteries. At this point, four endings of each interlobar artery were already visible, and later developed into the arcuate arteries. The branching pattern of the interlobar arteries was similar to a blueprint, because it was mostly constant and could be traced throughout all following states of development. One interlobar artery was somewhat longer than the other. This interlobar artery developed a bifurcation, with one branch remaining 'linear' and the second one developing a subsequent trifurcation. The branchings of the second, shorter interlobar artery were a bit more variable. In total, there were four branching ends,

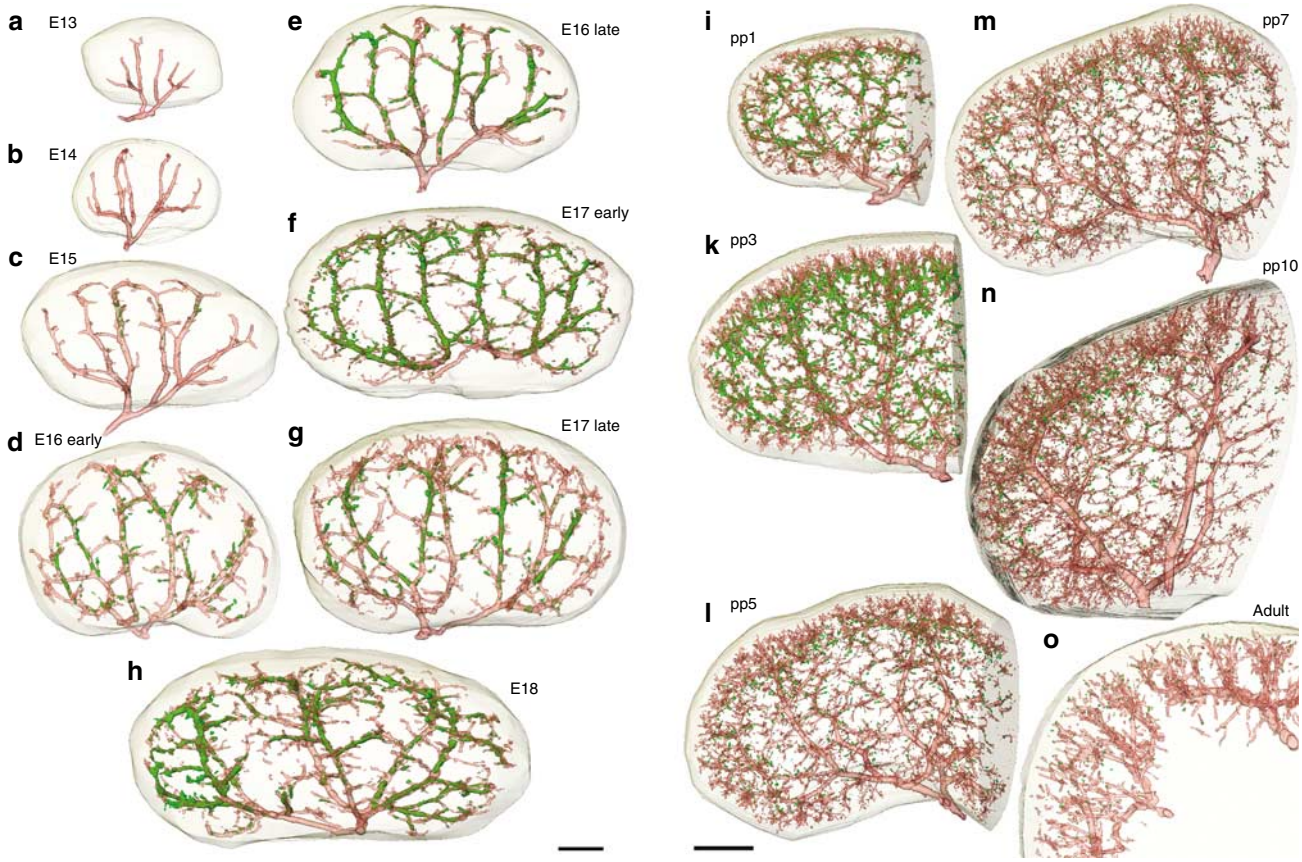

Figure 1 | Whole organ reconstruction of αSMA immunoreactive vascular structures (red) and of renin immunoreactive areas (green) in the developing mouse kidney. Bar = 300 μm for embryonic stages and 500 μm for postnatal (pp) stages. (**a**) Day E13, (**b**) day E14, (**c**) day E15, (**d**) early day E15, (**e**) late day E16, (**f**) early day E17, (**g**) late day E17, (**h**) day E18, (**i**) postnatal (pp) day 1, (**k**) postnatal (pp) day 3, (**l**) postnatal (pp) day 5, (**m**) postnatal (pp) day 7, (**n**) postnatal (pp) day 10, and (**o**) (adult) day 90.

which consisted of either a linear branch together with a trifurcation comparable to the situation on the contralateral side or of two subsequent bifurcations.

On day 14 (day E14) of development, the first signs of arc formation became visible in that the trunks of the arcuate arteries developed t-shaped caps at their distal ends, which spread toward each other, but which usually did not fuse and form anastomoses (Figure 1b). Few lateral buds along the arcuate trunks became visible. It is notable that in this context, the expression of αSMA was not always continuous along the vessel, but that islets of αSMA immunoreactivity also appeared, further outlining the development of the arcuate arteries.

Early on day 15 (day E15), the arcuate t-shaped caps had clearly developed and side branches also grew out from the arcuate trunks (Figures 1c and 2c). These side branches could be separated into two groups, namely afferent arterioles, which branched off from the concave side of the arcuate trunk, and which fed already developed glomeruli, and side-boughs, which branched off almost perpendicularly at the convex side of the arcuate trunk, which later formed the arcuate side arteries. Both types of branches were restricted to the arcuate arteries and were never seen in interlobar or renal arteries. By late day 15 of embryonic development, arc formation and the growth of arcuate side arteries had proceeded further (Figure 1d). The first ramifications of the arcuate side arteries forming the afferent arterioles of the juxtamedullary glomeruli became visible. These side branches of the arcuate trunks did not fuse with others to form anastomoses what could not always be clearly distinguished from two-dimensional projections because of overlapping projections. Apart from juxtamedullary afferent arterioles, the ramifications of the arcuate side arteries also give rise to cortical interlobular arteries later on.

The next day (day E16), growth and ramifications of the t-shaped caps were predominant impressed and also, the arcuate side arteries, which had increased in number, displayed high branching activity (Figures 1e, f, and 2b). The afferent arterioles arising from the arcuate main trunks had developed bifurcations, thus increasing the number of deep glomeruli being directly fed by the arcuate main trunks. A growing number of juxtamedullary afferent arterioles also developed from the arcuate side arteries. An increased number of αSMA immunoreactive islets, outlining the future development and ramifications of arcuate side arteries, was visible.

On day 17 of development (day E17), t-cap ramification continued, sending off juxtamedullary afferent arterioles. Now a clear vascular network below the subcapsular nephrogenic zone became apparent (Figures 1g and 2c). While the total number of arcuate side arteries branching off from the arcuate main trunks did not increase further, terminal branching of these side arteries forming juxtamedullary afferent arterioles continued.

Prior to birth (day E18), branching of arcuate side arteries continued. Existing afferent arterioles elongated (Figures 1h and 2d). The first signs of interlobular artery formation in the subcapsular zone became visible on the first day after birth (day pp1). At this stage, the t-shaped cap branches and the arcuate side arteries had developed further and had generated an increasing number of afferent arterioles, which grew crookedly in the layer around the renal medulla (Figures 1i and 2e; Supplementary File 1). Two days later (day pp3), the ramification of the arcuate t-cap and arcuate side arteries, and the development of afferent arterioles had continued (Figures 1k and 2f). Growing of corticoradial interlobular arteries was apparent. The first sprouting of afferent arterioles from interlobular arteries could be recognized. Five days after birth (day pp5), the ramifications of the arcuate side arteries were still maturating. Formation of corticoradial interlobular arteries rising from the arcuate t-cap and arcuate side arteries was predominant (Figures 1l and 2g). Numerous αSMA immunoreactive islets were visible, which later merged to form interlobular arteries and afferent arterioles. Also, 2 days later (day pp7), prominent formation of corticoradial interlobular arteries from the t-cap arteries impressed (Figures 1m and 2h). Similarly, in the arcuate side arteries, ramification, including formation of corticoradial interlobular arteries, continued. The ramifications of interlobular arteries refined. Mid-cortical afferent arterioles had further developed. Ten days after birth (day pp10), the system of interlobular and afferent arterioles in the subcortical zone had further maturated (Figures 1n and 2i), but was not yet identical to the adult stage, in which interlobular arteries imposed as radially sorted, lengthy structures from which afferent arterioles branched off (Figure 2a and b).

Efferent arterioles, in particular juxtamedullary ones, became visible by αSMA immunoreactivity, if at all, in juxtamedullary glomeruli.

Developmental changes of renin expression

Renin immunoreactivity in the metanephric tissue first appeared in association with blood vessels on early day 15 of embryonic development (Figures 1c and 2a). Intrarenal renin expression appeared with a spotted pattern in the distal part of the trunks of the arcuate arteries, regardless of whether they had already formed arcs. Although singular spots of renin immunoreactivity were also seen in developing arcuate side arteries, those side arteries and afferent arterioles of deep glomeruli were usually free of renin at that time (Figure 2a). At the end of day 15, renin expression began to expand in the trunk of the arcuate artery in a retrograde fashion, as well as in the more developed arcuate side arteries (Figure 1d). It should be noted that renin expression was not continuous along the vessels, and did not provide a clearly predictable pattern. This heterogeneity of renin expression also continued into the early part of day 16 of development, when, in addition, part of the juxtamedullary afferent arterioles branching off either directly from the arcuate trunks or from arcuate side arteries began to express renin at their terminal ends, that is, in the juxtaglomerular position

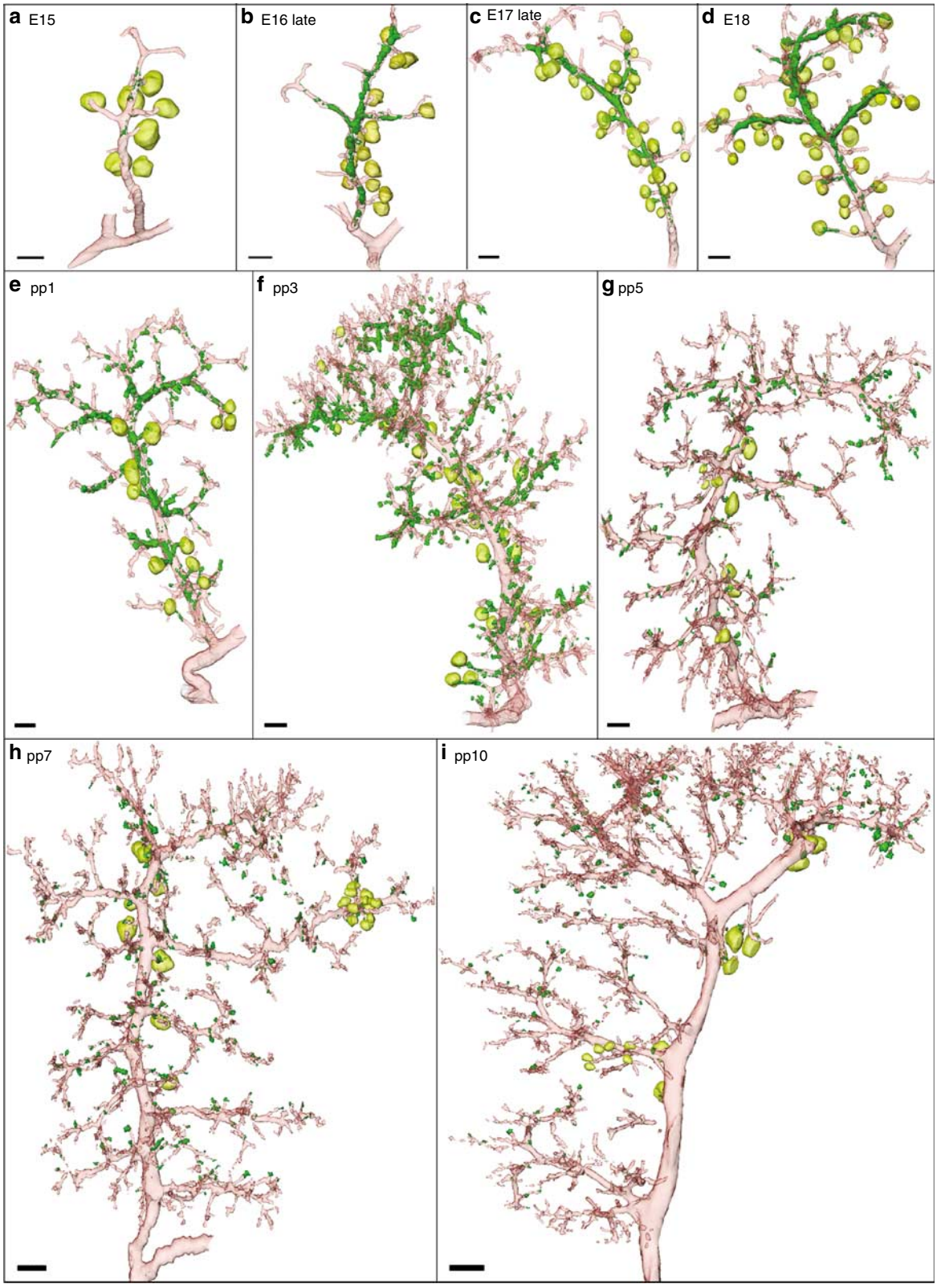

Figure 2 | Reconstruction of αSMA immunoreactive vascular structures (red) and of renin immunoreactive areas (green) in the developing 'linear' branch of arcuate arteries. Bar = 100 μm. (**a**) Day E15, (**b**) day E16, (**c**) day E17, (**d**) day E18, (**e**) postnatal (pp) day 1, (**f**) postnatal (pp) day 3, (**g**) postnatal (pp) day 5, (**h**) postnatal (pp) day 7, and (**i**) postnatal (pp) day 10.

(Figure 1e). At the end of embryonic day 16, renin was expressed throughout the trunks of the arcuate arteries and also many of the arcuate side arteries expressed renin in their proximal parts (Figure 1f). Although some afferent arterioles already expressed renin in the juxtaglomerular position, many of the existing afferent arterioles were mainly renin free. The tips of the branches of the arcuate side arteries were free of renin (Figure 2b). The next day (day E17), the strong renin expression in the arcuate trunk appeared to disperse in the orthograde (proximal to distal) direction. Renin expression now appeared in a more maculated fashion (Figure 1g). The majority of the existing afferent arterioles strongly expressed renin either along their whole length, as in afferent arterioles directly arising from the arcuate trunk, or in the juxtaglomerular position, as mainly in afferent arterioles arising from arcuate side arteries (Figure 2c). Renin expression in arcuate side arteries was not a constant characteristic, since substantial numbers of arcuate side arteries were devoid of renin. The developing ramifications of arcuate side arteries and developing afferent arterioles were free of renin. Close to birth (day E18), renin expression had disappeared from the proximal part (close to origin from interlobar artery) of the arcuate trunk and from proximal arcuate side arteries, including afferent arterioles arising in that region (Figures 1h and 2d). One day after birth (pp1), renin immunoreactivity had mainly disappeared from the arcuate trunks. Renin expression was now mainly found in thicker arcuate side arteries, where it imposed in a striped pattern, and in juxtamedullary afferent arterioles, which expressed renin more frequently, mainly at their juxtaglomerular ends (Figures 1i and 2e). Afferent arterioles newly developing from the arcs were mainly free of renin. Developing interlobular arteries in the subcapsular space were completely free of renin (Figure 2e). Two days later (pp3), renin expression in the arcuate trunks had disappeared and was also greatly reduced in the main branches of the arcuate side arteries (Figures 1k and 2f). In these vessels, renin expression had shifted from the proximal parts to the more distal ramifications, including afferent arterioles (Figure 2f). In many cases, renin expression was already restricted to the juxtaglomerular portion of afferent arterioles. The developing corticoradial interlobular arteries as well as subcapsular afferent arterioles spreading off were still free of renin. Five days after birth (pp5), renin was found only in mature afferent arterioles, mainly in a juxtaglomerular position (Figures 1l and 2g). The developing corticoradial interlobular arteries as well as afferent (cortical) arterioles developing in that region were free of renin (Figure 2g). Two days later (pp7), overall renin expression imposed with a spotted pattern, renin expression now being localized exclusively in afferent arterioles arising from arcuate side arteries, in particular at their terminal (juxtaglomerular) ends (Figures 1m and 2h). Developing subcapsular interlobular arteries as well as developing cortical afferent arterioles were still devoid of renin (Figure 2h). On the tenth day after birth (pp10), renin expression was found at the juxtaglomerular portion of afferent arterioles in the juxtamedullary and mid-cortical zones (Figures 1n and 2i). In the adult kidney, overall renin expression produced a spot pattern, in the way that renin expression was restricted to the terminal parts of the majority of afferent arterioles (Figure 1o). Renin expression in juxtamedullary afferent arterioles appeared to be lower than that in the other cortical zones.

Examination of renin expression at higher magnification made it clear that renin expression at any developmental stage occurred frequently in insulated cells that formed the inner media layer of the vessels (Figure 3a–c). We did not observe a predictable cellular pattern of renin expression, except when renin was expressed in the juxtaglomerular portions of afferent arterioles (Figure 3c and d). In particular, we found no special pattern of renin expression at existing or developing branchings (Figure 3a, c, and d). A major difference in the expression of renin in the different vessel segments was that it went in parallel to the expression of αSMA except in afferent arterioles, in which renin and αSMA expression occurred reciprocally (Figure 3c and d). The closer the cells were located to the vascular pole, the more renin and less αSMA they expressed. This phenomenon was not dependent on the maturation of the kidneys. It was apparent as soon as renin expression appeared in afferent arterioles at any developmental stage.

Quantification of renin expression during kidney development

Apparently, the number of individual vessels expressing renin increased during kidney development, while the relative coverage of individual vessels with renin decreased. To obtain an estimate of the quantity of the number of renin-expressing cells during kidney development, we determined the tissue volumes staining positive for renin. As shown in Figure 4a,

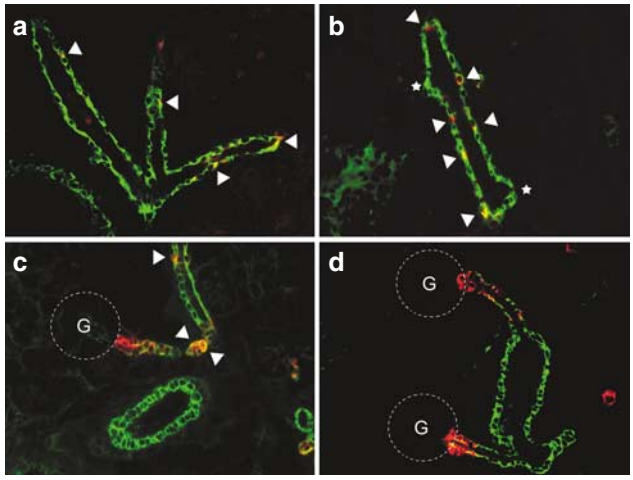

Figure 3 | αSMA immunoreactivity (red) and renin immunoreactive (green) in kidney sections of E15 (a), E17 (b), pp3 (c), and pp (d). Yellow color indicates overlap of αSMA and renin immunoreactivity. Original magnification × 400. G, glomerulus; arrowheads indicate cells expressing both αSMA and renin; asterisks indicate sprouting/branching buds.

the renin-positive volume increased steeply from day 15 of development until birth and then increased gradually but more moderately until the adult state. The renin volume 10 days after birth was close to that of adult kidneys. These time-dependent changes of renin-positive volumes were very similar to the changes of renin mRNA content during kidney development (Figure 4b). In contrast, whole kidney volume, which was calculated after subtraction of the volume of the renal pelvis, increased more exponentially during development (Figure 4c), that is, unlike with renin, there was not a clear flattening of the curve in the postnatal period. In contrast, kidney volume increased about sixfold between the tenth postnatal day and the adult state. Similarly, the volume staining positive for αSMA, which was considered to reflect the extension of the preglomerular arterial/arteriolar tree, increased more exponentially until final maturation of the kidney (Figure 4d), and thus paralleled the volume development of the whole kidney. αSMA immunoreactive tissue volumes were also calculated after subtraction of the renal pelvis, to eliminate the contribution of smooth muscle cells of the renal pelvis. It could be estimated from the volume data for the adult kidney, for example, that renin-expressing volumes comprised about 0.025% and αSMA-expressing volumes about 1% of the total kidney volume.

DISCUSSION

A number of studies have elaborated a body of knowledge about the development of metanephric kidneys in a variety of species. Most of these studies, however, have focused on the development of the collecting duct, tubule,[17] and particularly, glomerulus formation,[18–22] while markedly less is known about the development of the complex but well-organized intrarenal vasculature. There is evidence to indicate that the renal vasculature probably develops by a combination of vasculogenesis, that is, *de novo* differentiation of blood vessels, and angiogenesis, that is, sprouting of new vessels from already existing vessels. An essential starting event in this context is likely the metanephric induction of VEGF and Flt-1 expression leading to activation and/or maturation of endothelial cells.[23–27] The next essential step appears to be endothelial production of platelet-derived growth factor-β, (PDGF-β) causing the attraction of pericytes and smooth muscle cells to stabilize the newly formed vessel,[28–30] a process that also requires ephrin-2 function.[31,32] How the complex intrarenal vascular network is formed is not understood. There are findings to indicate that neurotrophic factors[33] and Notch[34] are relevantly involved, in addition to VEGF and PDGF. The complex branching pattern of the intrarenal vessels likely occurs via sprouting and intussusception.[35]

On a descriptive level, there is agreement that for the mammalian metanephric kidney,[16,36,37] the renal artery divides into a species-dependent number of interlobar branches, which in turn split into branches forming arcuate arteries. From there, the arcuate arteries branch off into interlobular arteries, which give rise to afferent arterioles feeding the capillary network of the glomeruli. To our knowledge, the present study is the first one that allows researchers to reconcile this developmental process for the mouse kidney by providing a three-dimensional perception of this process. One issue that became particularly evident from our study is the very active formation of the transversal arcuate side arteries, which do not form anastomoses with other branches. Our study also confirms the notion that

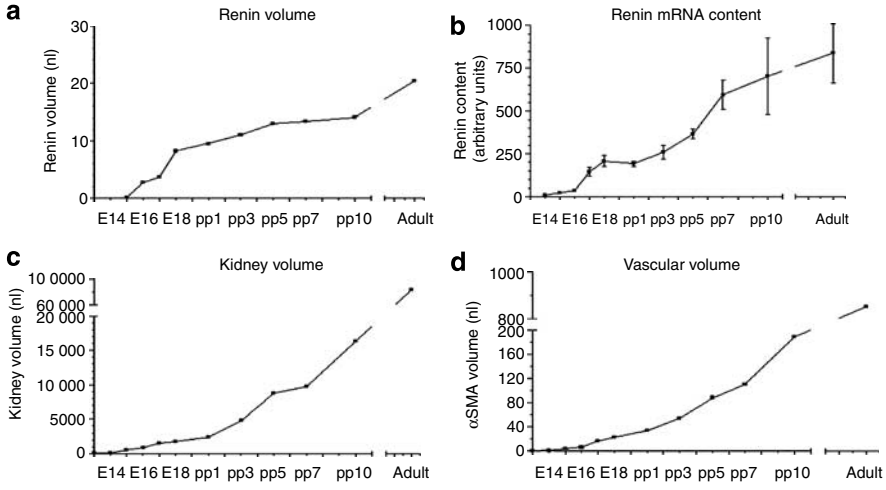

Figure 4 | Time-dependent changes of renin volume and renin in RNA, of kidney and vascular volume during kidney development. (**a**) Time course of calculated renin immunoreactive tissue volumes during development of the mouse kidney. Data are single values per time point. They were derived from the kidneys shown in Figure 1. Volume is given in voxel units. (**b**) Time course of renal renin mRNA content during development of the mouse kidney. Date are means ± s.e.m. of 3–5 kidneys per time point. The calculation of the data is explained in the Materials and Methods section. (**c**) Time course of calculated kidney volumes (after subtraction of renal pelvis volume) during development of the mouse kidney. Data are single values per time point. They were derived from the kidneys shown in Figure 1. Volume is given in voxel units. (**d**) Time course of calculated αSMA immunoreactive tissue volumes (after subtraction of renal pelvis area) during development of the mouse kidney. Data are single values per time point. They were derived from the kidneys shown in Figure 1. Volume is given in voxel units.

vessel formation and growth in the rodent kidney occur until the state of adulthood has definitively been reached.[38] The observation of islets of αSMA immunoreactivity, which already provide a clue of the future curvature of the complete vessel, supports the assumption that the expression of αSMA is secondary to the formation of the vessels, including their stable walls.[38]

As to the intrarenal development of renin expression, which was the main objective of this study, our study confirms that intrarenal renin expression in the mouse kidney starts around the fifteenth day of development.[6,8] Our data are in agreement with the findings and models presented by previous publications, in particular those of Jones *et al.*[8] and Kon *et al.* for mice[6] and of Gomez *et al.* for rats.[7] However, in contrast to other studies, we could not find renin expression in either the renal artery, the interlobar arteries, or outside of vessel structures containing αSMA, which could be due to species or strain differences or to a lower sensitivity of our renin antibody. According to our observations, renin expression starts in the distal arcuate artery trunks and expands there in a retrograde fashion but retracts in a retrograde direction. Renin expression in arcuate t-cap and arcuate side arteries developed and retracted in a retrograde direction. Vascular regions with the highest growth and branching activity were devoid of renin expression. It appears therefore as if renin expression does not occur until the functional vessel wall is formed, as indicated by the expression of αSMA. A preferential expression of renin at branching points, as found for mature rat kidneys,[15] was not evident from our data. It could therefore be concluded that the expression of renin at branching points of mature preglomerular vessels is a species-specific phenomenon. We found it remarkable that the development of interlobular arteries into the nephrogenic zone (subcapsular zone) was not associated with major renin expression. However, once afferent arterioles had developed, they strongly expressed renin. Finally, in the adult kidney, renin expression was localized at the typical juxtaglomerular position. The observation that renin expression appeared and disappeared in the more maturated vessel walls is in accordance with the observation that renin expression is not a prerequisite for the proper developmental formation of the intrarenal arterial vessel tree.[39]

Nonetheless, renin-deficient mice develop tubular structural defects and vascular thickenings in the juvenile and adult state, a phenomenon that can be mimicked by general interference with the renin–angiotensin system.[40,41] Since all components of the renin–angiotensin system are already expressed in the fetus,[42] it appears therefore as if the developmental regulated renin expression is relevant for the kidney development, although details of this function still await further elucidation.[43]

Although renin expression in the adult kidney appears as a rather rare event at first glance when compared with developing kidneys, our data illustrate that the number of renin-expressing cells is highest in the adult kidney, which is also confirmed by the estimation of the total renin mRNA content in the kidneys at different developmental stages. For completeness, it should be added in this context that the relative abundance of renin expression (i.e., ratio of renin volume/kidney volume) reaches a maximum shortly after birth and then declines, which is also in accordance with findings by others.[4,11,44] From the parallel changes of renin immunoreactive volumes and renin mRNA content, leading to an almost constant ratio of renin mRNA over the volume of renin immunoreactive cells for any developmental stage, one may infer that changes of renin gene expression during development result mainly from switch on and switch off of renin gene transcription in individual cells.

All these different aspects, as listed above, lead to the impression that the characteristic developmental changes of intrarenal renin expression result from the specific spatio-temporal pattern of a yet unidentified direct activator of renin gene expression, rather than from the switching on and off of developmentally relevant transcription factors in the walls of preglomerular arteries.[13] In fact, it has already been speculated that the developmental changes of intrarenal renin expression may be related to the development of sympathetic nerves.[13] It should be furthermore mentioned in this context that the expression of the type II receptor of TGF-β changes in pattern, which is strikingly identical to that of renin expression during kidney development.[45]

To identify and verify the essential factors triggering developmental renin expression, it is of interest now to study the development of intrarenal renin expression in mice with defined gene mutations, using the results of this study as a reference system. Obvious candidates in this context will be β-adrenergic receptors as well as the type II receptor of TGF-β.

MATERIALS AND METHODS

Immunohistochemistry for renin and α-smooth muscle actin

All animal experiments were conducted according to the National Institutes of Health guidelines for the care and use of animals in research.

Kidneys were sampled from fetuses 13, 14, 15, 16, 17, and 18 days after formation of vaginal plugs (day E0), from 1-, 3-, 5-, 7-, and 10-day-old pubs and from adult C57/Bl6 (Charles River, Sulzfeld, Germany) mice.

After killing the mice, one kidney from each subject was dissected and fixed for 24 h in 4°C methyl Carnoy's solution (60% methanol, 30% chloroform, and 10% glacial acetic acid) for the histological preparation as described previously,[46] while the other kidney was stored at −80°C until RNA isolation. Kidneys from adult mice were perfusion fixed with 4% paraformaldehyde. The fixed kidneys were dehydrated by a graded series of alcohol solutions (two times 70, 80, 90, and 100% methanol), followed by 100% isopropanol for 0.5 h each and embedded in paraffin.

Immunolabeling was performed on 5-μm paraffin sections. After blocking with 3% H_2O_2 in methanol for 20 min and with 10% horse serum/1% bovine serum albumin in phosphate-buffered saline for 0.5 h at room temperature, sections were incubated with chicken anti-renin IgG (diluted 1:200; Davids Biotechnologie GmbH, Regensburg, Germany) and mouse anti-αSMA IgG (diluted 1:100; Beckman Coulter-Immunotech, Krefeld, Germany) overnight at

4°C. After several washing steps and blocking with phenylhydrazine, the sections were incubated with Cy2-conjugated donkey anti-chicken IgG and rhodamine (TRITC)-conjugated donkey anti-mouse IgG fluorescent antibodies (Dianova, Hamburg, Germany) for 2 h and mounted with glycergel (DakoCytomation, Glostrup, Denmark).

Three-dimensional reconstruction

Serial sections of kidney specimens were fixed and stained for renin and for αSMA as described above. Digitalization of the serial slices was performed using an AxioCam MRm camera (Zeiss, Jena, Germany) mounted on an Axiovert200M microscope (Zeiss) with fluorescence filters for renin and αSMA (TRITC: filter set 43: Cy2: filter set 38 HE; Zeiss). After acquisition, a stack of equal-sized images was built using the graphic tool ImageJ (Wayne Rasband, NIH, Bethesda, MD, USA). The equalized data were then imported into the Amira 4.1 visualization software (Mercury Computer Systems Inc., Chelmsford, MA, USA) on a Dell Precision 690 computer system (Dell, Frankfurt, Germany), and subsequently split into the renin and αSMA channels. After this step, the renin and αSMA channels were aligned. In the segmentation step, the αSMA and renin data sets served as a scaffold and were spanned manually or automatically using grayscale values. Matrixes, volume surfaces, and statistics were generated from these segments.

Semiquantification of renin mRNA by real-time PCR

Total RNA was isolated from the frozen kidneys as described by Chomczynski and Sacchi[47] and quantified by a photometer. One microgram of the resulting RNA was used for reverse transcriptase (RT)-PCR. The cDNA was synthesized by MMLV reverse transcriptase (Superscript-Invitrogen, Carlsbad, CA, USA). For quantification of renin mRNA expression (sense: 5′-ATGAAGGGG GTGTCTGTGGGGTC-3′, antisense: 5′-ATGCGGGGAGGGTGGG CACCTG-3′), real-time RT-PCR was performed using a Light Cycler Instrument (Roche Diagnostics Corp., Basel, Suisse) and the QuantiTect SYBR Green PCR kit (Qiagen, Hilden, Germany), with GAPDH (sense: 5′-TTCATTGACCTCAACTACAT-3′, antisense: 5′-GAGGGGCCATCCACAGTCTT-3′) as a control. PCR was run for 30 cycles with 15 s per 95°C denaturation, 20 s/58°C annealing and 20 s/72°C elongation. To verify the accuracy of the amplicon, a melting curve analysis was done after amplification.

Total renin mRNA content per kidney was calculated from the yield of RNA extracted from the whole kidneys times the renin mRNA estimate obtained from the defined amount of RNA used for RT-PCR real time measurement. For the RT-PCR real-time measurements, a pool of RNA from adult mouse kidneys was generated, which served as standard for all RT-PCR runs. Thus, all renin mRNA levels for the developing kidneys were estimated relative to the levels in adult kidneys.

DISCLOSURE

The authors state no conflict of interest.

ACKNOWLEDGMENTS

The expert technical assistance provided by Anna B'angui and Susanne Lukas is gratefully acknowledged. This study was financially supported by the Deutsche Forschungsgemeinschaft (SFB 699).

REFERENCES

1. Kon Y. Comparative study of renin containing cells. Histological approaches. *J Vet Med Sci* 1999; **61**: 1075–1086.
2. Phat VN, Camilleri JP, Bariety J *et al.* Immunohistochemical characterization of renin-containing cells in the human juxtaglomerular apparatus during embryonal and fetal development. *Lab Invest* 1981; **45**: 387–390.
3. Minuth M, Hackenthal E, Poulsen K *et al.* Renin immunocytochemistry of the differentiating juxtaglomerular apparatus. *Anat Embryol* 1981; **162**: 173–181.
4. Drukker A, Donoso VS, Linshaw MA *et al.* Intrarenal distribution of renin in the developing rabbit. *Pediatr Res* 1983; **17**: 762–765.
5. Gomez RA, Lynch KR, Chevalier RL *et al.* Renin and angiotensinogen gene expression in maturing rat kidney. *Am J Physiol* 1988; **254**: F582–F587.
6. Kon Y, Hashimoto Y, Kitagawa H *et al.* An immunohistochemical study on the embryonic development of renin-containing cells in the mouse and pig. *Anat Histol Embryol* 1989; **18**: 14–26.
7. Gomez RA, Lynch KR, Sturgill BC *et al.* Distribution of renin mRNA and its protein in the developing kidney. *Am J Physiol* 1989; **257**: F850–F858.
8. Jones CA, Sigmund CD, McGowan RA *et al.* Expression of murine renin genes during fetal development. *Mol Endocrinol* 1990; **4**: 375–383.
9. Graham PC, Kingdom JC, Raweily EA *et al.* Distribution of renin-containing cells in the developing human kidney: an immunocytochemical study. *Br J Obstet Gynaecol* 1992; **99**: 765–769.
10. Dodge AH. Sites of renin production in fetal, neonatal and postnatal Syrian hamster kidneys. *Anat Rec* 1993; **235**: 144–150.
11. Carbone GM, Sheikh AU, Rogers S *et al.* Developmental changes in renin gene expression in ovine kidney cortex. *Am J Physiol* 1993; **264**: R591–R596.
12. Kon Y, Alcorn D, Murakami K *et al.* Immunohistochemical studies of renin-containing cells in the developing sheep kidney. *Anat Rec* 1994; **239**: 191–197.
13. Pupilli C, Gomez RA, Tuttle JB *et al.* Spatial association of renin-containing cells and nerve fibers in developing rat kidney. *Pediatr Nephrol* 1991; **5**: 690–695.
14. Fischer E, Schnermann J, Briggs JP *et al.* Ontogeny of NO synthase and renin in juxtaglomerular apparatus of rat kidneys. *Am J Physiol* 1995; **268**: F1164–F1176.
15. Reddi V, Zaglul A, Pentz ES *et al.* Renin-expressing cells are associated with branching of the developing kidney vasculature. *J Am Soc Nephrol* 1998; **9**: 63–71.
16. Gomez RA, Norwood VF, Tufro-McReddie A. Development of the kidney vasculature. *Microsc Res Tech* 1997; **39**: 254–260.
17. Saxen L, Lehtonen E. Embryonic kidney in organ culture. *Differentiation* 1987; **36**: 2–11.
18. Spinelli F. Structure and development of the renal glomerulus as revealed by scanning electron microscopy. *Int Rev Cytol* 1974; **39**: 345–378.
19. Kazimierczak J. A study of scanning (SEM) and transmission (TEM) electron microscopy of the glomerular capillaries in developing rat kidney. *Cell Tissue Res* 1980; **212**: 241–255.
20. Bertram JF. Analyzing renal glomeruli with the new stereology. *Int Rev Cytol* 1995; **161**: 111–172.
21. Robert B, Abrahamson DR. Control of glomerular capillary development by growth factor/receptor kinases. *Pediatr Nephrol* 2001; **16**: 294–301.
22. Ballermann BJ. Glomerular endothelial cell differentiation. *Kidney Int* 2005; **67**: 1668–1671.
23. Tufro-McReddie A, Norwood VF, Aylor KW *et al.* Oxygen regulates vascular endothelial growth factor-mediated vasculogenesis and tubulogenesis. *Dev Biol* 1997; **183**: 139–149.
24. Kitamoto Y, Tokunaga H, Tomita K. Vascular endothelial growth factor is an essential molecule for mouse kidney development: glomerulogenesis and nephrogenesis. *J Clin Invest* 1997; **99**: 2351–2357.
25. Robert B, St John PL, Abrahamson DR. Direct visualization of renal vascular morphogenesis in Flk1 heterozygous mutant mice. *Am J Physiol* 1998; **275**: F164–F172.
26. Tufro A, Norwood VF, Carey RM *et al.* Vascular endothelial growth factor induces nephrogenesis and vasculogenesis. *J Am Soc Nephrol* 1999; **10**: 2125–2134.
27. Mattot V, Moons L, Lupu F *et al.* Loss of the VEGF(164) and VEGF(188) isoforms impairs postnatal glomerular angiogenesis and renal arteriogenesis in mice. *J Am Soc Nephrol* 2002; **13**: 1548–1560.
28. Lindahl P, Hellstrom M, Kalen M *et al.* PDGF-Rbeta signaling controls mesangial cell development in kidney glomeruli. *Development* 1998; **125**: 3313–3322.
29. Hellstrom M, Kalen M, Lindahl P *et al.* Role of PDGF-B and PDGFR-beta in recruitment of vascular smooth muscle cells and pericytes during embryonic blood vessel formation in the mouse. *Development* 1999; **126**: 3047–3055.
30. Eng E, Holgren C, Hubchak S *et al.* Hypoxia regulates PDGF-B interactions between glomerular capillary endothelial and mesangial cells. *Kidney Int* 2005; **68**: 695–703.

31. Takahashi T, Takahashi K, Gerety S *et al.* Temporally compartmentalized expression of ephrin-B2 during renal glomerular development. *J Am Soc Nephrol* 2001; **12**: 2673–2682.
32. Foo SS, Turner CJ, Adams S *et al.* Ephrin-B2 controls cell motility and adhesion during blood–vessel–wall assembly. *Cell* 2006; **124**: 161–173.
33. Kloth S, Suter-Crazzolara C. Modulation of renal blood vessel formation by glial cell line-derived neurotrophic factor. *Microvasc Res* 2000; **59**: 190–194.
34. McCright B, Gao X, Shen L *et al.* Defects in development of the kidney, heart and eye vasculature in mice homozygous for a hypomorphic Notch2 mutation. *Development* 2001; **128**: 491–502.
35. Makanya AN, Stauffer D, Ribatti D *et al.* Microvascular growth, development, and remodeling in the embryonic avian kidney: the interplay between sprouting and intussusceptive angiogenic mechanisms. *Microsc Res Tech* 2005; **66**: 275–288.
36. Lewis OJ. The development of the blood vessels of the metanephros. *J Anat* 1958; **92**: 84–97.
37. Kazimierczak J. Topography and structure of vasculature in developing cortex of rat kidney. *Anat Embryol* 1978; **153**: 213–226.
38. Carey AV, Carey RM, Gomez RA. Expression of alpha-smooth muscle actin in the developing kidney vasculature. *Hypertension* 1992; **19**(Suppl 2): II168–II175.
39. Takahashi N, Sequeira Lopez ML, Cowhig Jr JE *et al.* Ren1c homozygous null mice are hypotensive and polyuric, but heterozygotes are indistinguishable from wild-type. *J Am Soc Nephrol* 2005; **16**: 125–132.
40. Tufro-McReddie A, Romano LM, Harris JM *et al.* Angiotensin II regulates nephrogenesis and renal vascular development. *Am J Physiol* 1995; **269**: F110–F115.
41. Gomez RA, Norwood VF. Developmental consequences of the renin–angiotensin system. *Am J Kidney Dis* 1995; **26**: 409–431.
42. Schutz S, Le Moullec JM, Corvol P *et al.* Early expression of all the components of the renin–angiotensin-system in human development. *Am J Pathol* 1996; **149**: 2067–2079.
43. Matsusaka T, Miyazaki Y, Ichikawa I. The renin angiotensin system and kidney development. *Annu Rev Physiol* 2002; **64**: 551–561.
44. Gomez RA, Pupilli C, Everett AD. Molecular and cellular aspects of renin during kidney ontogeny. *Pediatr Nephrol* 1991; **5**: 80–87.
45. Liu A, Ballermann BJ. TGF-beta type II receptor in rat renal vascular development: localization to juxtaglomerular cells. *Kidney Int* 1998; **53**: 716–725.
46. Mann B, Hartner A, Jensen BL *et al.* Acute upregulation of COX-2 by renal artery stenosis. *Am J Physiol* 2001; **280**: F119–F125.
47. Chomczynski P, Sacchi N. Single-step method of RNA isolation by acid guanidinium thiocyanate–phenol–chloroform extraction. *Anal Biochem* 1987; **162**: 156–159.